# THREE-DIMENSIONAL STRUCTURE OF GAP JUNCTIONS IN FRAGMENTED PLASMA MEMBRANES FROM RAT LIVER

SANTOSH S. SIKERWAR AND NIGEL UNWIN
*Department of Cell Biology, Stanford University School of Medicine, Stanford, California 94305*

ABSTRACT Gap junctions forming extensive hexagonal crystalline sheets (unit cell dimension, $a = 89$ Å) were obtained by mild mechanical disruption of plasma membranes from rat liver. The sheets were analysed in three dimensions by negative stain electron microscopy and Fourier image processing. The crystallographic symmetry was shown to approximate to the two-sided plane group p622, indicating that the sheets are composed of two equivalent, oppositely-facing membrane assemblies. The structure of the connexon in these near-to-native junctions is essentially the same as that found in detergent-extracted junctions, the subunits appearing slightly tilted tangential to the central six-fold axis and aligned almost perpendicular to the membrane plane.

## INTRODUCTION

Gap junctions are plasma membrane specializations, which allow transfer of small molecules between the interiors of juxtaposed cells. Studies of their structure by a variety of techniques has shown them to be composed of arrays of annular units (18, 19), connexons, the central axes of which delineate the presumed paths for these molecules to diffuse (5, 17). The connexon is itself an assembly of six identical transmembrane subunits (5, 20), and the complete ~150 Å-long intercellular pathway is formed by a pair of them, coaxially aligned and linked together across the narrow space separating the plasma membranes of the connected cells. Electron microscopy of junctions isolated with detergent suggests that the connexon subunits are approximately rod-shaped and aligned almost perpendicular to the membrane plane with a slight tilt tangential to the central six-fold axis (20, 21). Several other details of the quaternary structure have been deduced, based on analysis of x-ray diffraction intensities from oriented gap junction pellets (12–14).

The appearance of the connexon within the native lipid environment is of particular interest because the detergent extraction procedures (7, ,8, 10, 16, 23) and alkaline treatment (10) normally used to isolate the junctions lead to packing changes (6) and may also affect the subunit structure. For example, the protein protruding from the cytoplasmic or extracellular membrane surfaces may be partially denatured by the detergent or high pH, resulting in a misleading representation of the functional assembly. The tilting of the connexon subunits around the channel may be altered by the tighter packing caused by chemical extraction of the lipid molecules. Here we report on the low resolution three-dimensional structure of the connexons in plasma membranes which have been perturbed only by mild mechanical treatment. Under these near-to-native conditions, the connexons have a greater center-to-center separation and pack more symmetrically in the crystal lattice than under most other conditions, but their structure is essentially the same as that described earlier (20, 21).

## METHODS

### Isolation of Plasma Membranes

All manipulations were carried out on ice using reagent grade chemicals and deionized glass distilled water.

The plasma membrane fraction was isolated from the livers of 8–10 rats (Sprague-Dawley, Madison, WI) of 140–160 g body weight, according to the procedure described earlier (23) with minor modifications. After excision, livers were pooled and washed in saline (0.9% (wt/vol) NaCl, 0.5 mM phenylmethyl-sulphonyl fluoride (PMSF), 1 mM dithiothreitol (DTT), and 5 mM sodium bicarbonate, pH 8.0). They were transferred to isolation buffer (0.5 mM ethyleneglycol-bis-$\beta$-aminoethyl ether (EGTA), 1 mM $MgCl_2$, 0.5 mM PMSF, 1 mM DTT, 4% (wt/wt) sucrose and 10 mM sodium bicarbonate, pH 8.0), cut into small pieces and homogenized in 20 ml portions using a Dounce homogenizer with a loose fitting teflon pestle. Subsequent steps to obtain the plasma membrane fraction were essentially as described (23), except that the final pellet from the 41% (wt/wt) step sucrose gradient was resuspended at a concentration of 2 mg protein/ml in: 1 mM $CaCl_2$, 1 mM DTT, 0.5 mM PMSF, 0.02% (wt/vol) sodium azide, 5 mM sodium bicarbonate, pH 7.6, using deuterium oxide, rather than water, as the solvent. This suspension was divided into 1 ml aliquots and kept on ice for periods of up to 3 d.

### Mechanical Disruption

The gap junction plaques were separated from the nonjunctional membranes by shearing. ~40 $\mu$l samples of the plasma membrane suspension

Please address all correspondence to Dr. Unwin at his present address: MRC Laboratory of Molecular Biology, Hills Road, Cambridge CB2 2QH, England.

were diluted to ~260 μl with deuterium oxide, passed several times through a gauge 30 G needle, and then successively through two glass capillaries (of internal bore ~200 μm and ~100 μm respectively). The sheared suspension was immediately centrifuged (1,750 *g* for 5 min) in 25 μl portions onto carbon support grids, for visualization in the electron microscope.

Large domains of hexagonally packed connexons were apparent in gap junctions prepared in this way. The most ordered sheets (e.g., Fig. 1) were obtained by incubating the isolated plasma membranes for 2 or 3 d before the mechanical disruption. Well-ordered gap junctions were also obtained after applying protocols other than the one described (using, for example, other low salt buffers, or water instead of deuterium oxide), but were less frequent. Thus deuterium oxide appears to play a significant role in the ordering process, which is presumably related to its effect of stabilizing hydrophobic interactions (8).

## Electron Microscopy and Image Processing

The carbon support grids were glow discharged in amylamine vapor before the deposition of the specimen, and negative staining was done with 2% (wt/vol) uranyl acetate. Electron microscopy was performed at a nominal magnification of 43,000X, using a Philips EM400 (Philips Electronic Instruments, Inc., Mahwah, NJ) operating at 100 KV. Tilting of specimens to provide the data for three-dimensional analysis was accomplished with a goniometer stage (using bent grids to achieve tilt angles of up to 71.5°). The orientation of the grid in the specimen holder was kept the same so that the specimen was always on the same side of the support film relative to the electron source. Accurate values for the tilt angles and axes were obtained using images of specimens tilted at two different angles, as described in reference 4. Actual magnifications were measured using catalase crystals as a calibration standard (22). Images were recorded on Kodak S0163 film, which was developed for 9 min in concentrated Kodak D19 developer.

Care was taken to minimize radiation damage by focussing on an area adjacent to the one of interest. The total dose in recording each micrograph was ~10 electrons/Å$^2$, and no more than two tilt values (total accumulated electron dose ~20 electrons/Å$^2$) were recorded for each specimen.

Micrographs were assessed both visually and by optical diffraction before analysis by computer and possible incorporation into the three-dimensional data sets. We rejected images in which the connexons were not distinctly visible, since weak staining is likely to introduce artifacts by giving unequal emphasis to different parts of the structure (24). We also ensured a maximum signal/noise ratio by rejecting those images for which the diffraction from areas containing ~500 connexons was significantly weaker than the examples in Fig. 2. Images of untilted specimens selected by these criteria always displayed good mirror symmetry, in contrast to the situation with junctions which have been treated with high concentrations of detergent (3, 6).

The selected regions of the micrographs were scanned at 25 μm intervals with a Perkin Elmer automatic microdensitometer having an aperture size of 25 μm, corresponding to 7 Å at the specimen. The two-dimensional arrays of optical densities thus generated were made up to 512 × 512 element size for Fourier transformation and subsequent measurement of the peak amplitudes and phases (2). The Fourier terms derived from images taken at different tilt angles were combined cumulatively according to the symmetry of the two-sided plane group p6, using a comparison range along the lattice lines of 0.0025 Å$^{-1}$. Typical phase errors from the 39 images of tilted specimens, based on comparisons between each new measurement and all previously accumulated phases related by symmetry, were 5–12°. Further details of the three-dimensional dataset are given in Table I. Curves were fitted to the data along the lattice lines by a least-squares method with the amplitude variations weighted according to the reliability of corresponding phases (1). The Fourier terms for synthesising the three-dimensional map were obtained by sampling the lattice lines at regular intervals (0.0025 Å$^{-1}$).

TABLE I
THREE-DIMENSIONAL DATA SET FROM IMAGES OF GAP JUNCTIONS IN PLASMA MEMBRANES

| Tilt angle | Tilt* axis | Phase‡ error | Number of comparisons |
|---|---|---|---|
| 0.0§ | 0.0 | — | — |
| 6.0 | 0.1 | 8.3 | 13 |
| 6.0 | 27.0 | 7.9 | 15 |
| 10.0 | 20.0 | 7.7 | 13 |
| 11.0 | 13.0 | 5.3 | 14 |
| 11.0 | 36.0 | 6.0 | 14 |
| 11.0 | 13.0 | 11.2 | 15 |
| 10.0 | 17.0 | 10.8 | 14 |
| 12.0 | 12.0 | 9.7 | 15 |
| 16.0 | 78.0 | 8.5 | 14 |
| 18.0 | 96.0 | 9.4 | 14 |
| 19.0 | 36.0 | 7.2 | 13 |
| 23.0 | 17.0 | 3.6 | 12 |
| 23.0 | 21.0 | 4.4 | 13 |
| 22.0 | 10.0 | 12.5 | 15 |
| 29.0 | 13.0 | 9.7 | 10 |
| 28.5 | 76.0 | 6.6 | 11 |
| 29.0 | 40.5 | 7.6 | 10 |
| 29.0 | 174.0 | 11.5 | 13 |
| 29.0 | 133.0 | 11.7 | 12 |
| 32.0 | 97.0 | 7.1 | 15 |
| 31.0 | 139.0 | 5.9 | 12 |
| 31.0 | 15.0 | 11.1 | 12 |
| 33.0 | 145.0 | 7.1 | 13 |
| 37.0 | 14.0 | 9.0 | 11 |
| 39.0 | 19.0 | 7.1 | 11 |
| 41.0 | 135.5 | 9.1 | 11 |
| 41.0 | 178.0 | 7.3 | 10 |
| 41.0 | 12.0 | 11.9 | 10 |
| 43.0 | 140.0 | 6.5 | 10 |
| 43.0 | 16.0 | 8.1 | 9 |
| 45.0 | 132.0 | 4.0 | 10 |
| 49.0 | 14.0 | 5.2 | 9 |
| 49.0 | 17.0 | 7.4 | 8 |
| 56.0 | 91.5 | 5.0 | 5 |
| 57.0 | 94.5 | 4.0 | 5 |
| 60.0 | 129.0 | 2.2 | 5 |
| 66.5 | 101.5 | 7.9 | 4 |
| 67.5 | 91.5 | 1.0 | 4 |
| 71.5 | 99.0 | 0.1 | 2 |

*Tilt angles and axes in degrees, the axes being measured relative to the [1,0] direction.
‡Average phase error in degrees, based on cumulative comparisons of image phases with others within 0.0025 Å$^{-1}$ along the lattice lines.
§Projection data include amplitudes and phases averaged from six images.

# RESULTS

## Gap Junctions in Plasma Membrane Fragments

Gap junctions isolated by mild mechanical disruption (see Methods), contain extensive crystalline arrays of connexons, often with fragments of the apposed plasma membranes still attached (Fig. 1). The connexons are organised on a hexagonal lattice with a center-to-center separation of

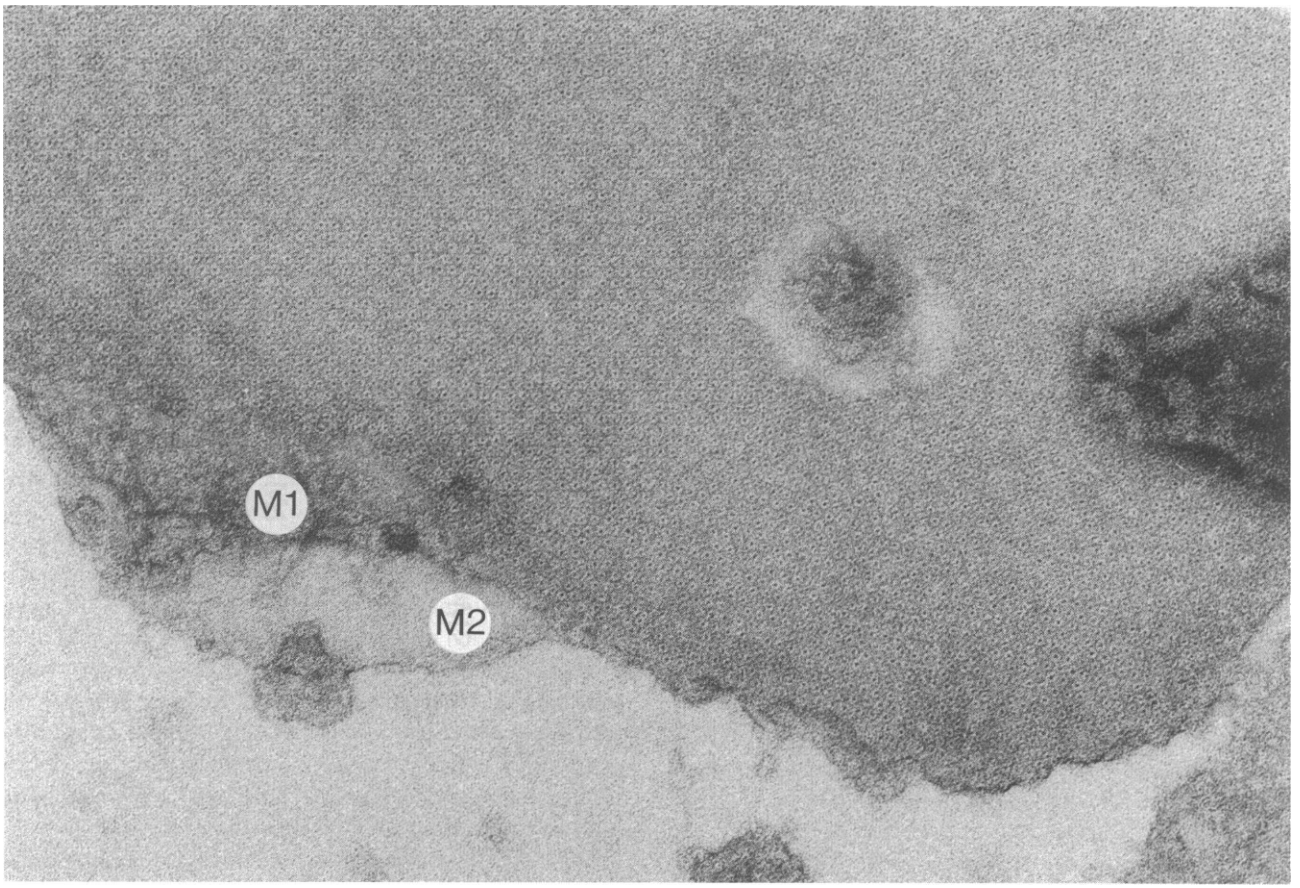


FIGURE 1. A gap junction plaque prepared by mild mechanical disruption of isolated plasma membranes. The plaque is composed of extensive hexagonal arrays of connexons, with fragments of the apposed plasma membranes (M1 and M2) still attached. Uranyl acetate stain. Magnification: ×214,000.

about 89 Å (89.0 Å ± 1.4 s.d. from measurement of 10 plaques), which is significantly greater than that usually obtained after isolation by detergent extraction (3, 5, 7).

## Diffraction Patterns

Diffraction patterns from images of the untilted junctions (Fig. 2) characteristically exhibit equally strong (1, 2) and (2, 1) reflections (indicating good mirror symmetry) and weak (1, 0) reflections.

The lattice line curves (Fig. 3), obtained by combining images of tilted junctions assuming the symmetry p6 (see Methods) show a small degree of scatter, particularly in the phases, indicating that the image details are very reproducible. The (1, 2) and (2, 1) lattice lines have similar amplitudes, but nearly opposite phases, consistent with the higher symmetry, p622, relating the two oppositely facing halves of the junction by dyad axes in its central plane.

## Three-Dimensional Map

The three-dimensional map synthesised from the Fourier terms along the lattice lines shows similar details as found previously (20). There is a region around the central plane of the junction (extracellular portion) which is strongly contrasted by the stain, two regions on either side (membrane-spanning portions) which are rather featureless, and two regions most distant from the central plane (the cytoplasmic faces) which are contrasted by the stain, but only weakly. Fig. 4 plots the contrast variation perpendicular to the plane of the junction, determined by measuring the difference between the maximum and minimum densities in sections at various levels throughout the structure. The width of the strong central peak is ~30 Å, indicating that the two apposed membranes are separated by about this amount. The two peaks associated with the cytoplasmic faces are on either side of this peak, each at a distance of ~60 Å, suggesting that the total thickness of the structure is not much more than 120 Å. While these dimensions are somewhat smaller than one would expect on the basis of x-ray diffraction measurements (12–14), there is almost certainly some shrinkage of the structure in this direction as a result of drying of the stain and radiation damage.

Fig. 5 illustrates the appearance of sections through the three-dimensional map parallel to the membrane plane. Clear details of the subunit structure of the connexon are

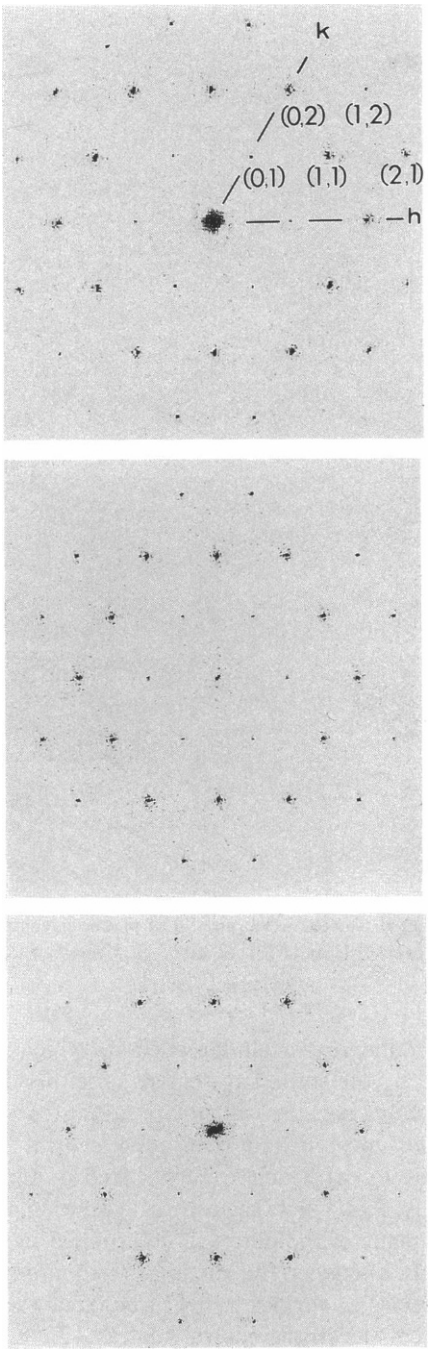


FIGURE 2. Computed diffraction patterns corresponding to well-ordered areas within plaques as in Fig. 1. These patterns almost invariably exhibit good mirror symmetry, indicated by equally strong (1, 2) and (2, 1) reflections. The indexing for one of the patterns is shown. Scale: 1 cm = 0.011 $Å^{-1}$.

visible in both the upper (Fig. 5 *a*) and lower (Fig. 5 *b*) membranes, and the features are similar in either case. The six subunits together produce only weak density modulations in the extracellular region, but are strongly contrasted there against the external environment and the central ~25 Å diameter channel. The subunits produce more pronounced modulations on the cytoplasmic surfaces, but the overall contrast there is weak. The azimuthal position of the subunits, represented by the peaks of density around the channel, are different on opposite sides of the membrane, indicating that the subunits are tilted tangential to the six-fold axis. The minimum angular difference is 24° in Fig. 5 *a* and 13° in Fig. 5 *b*, consistent with the inclination of the subunits being small (5–10°), although the stain embedding does not allow their paths through the membranes to be traced accurately.

## DISCUSSION

Conventional procedures for gap junction isolation are based upon the observation that gap junctions are relatively resistant to treatment with certain detergents (7, 9, 11, 16, 23) and alkaline extraction (10), which disrupt and remove the nonjunctional plasma membranes. Here, we used mild mechanical treatment to prepare the junctions, eliminating the chemical treatments altogether and permitting us to examine the structure within the original plasma membranes. Of particular interest was the structure of the connexon, which has not hitherto been investigated in three-dimensions embedded in a native lipid environment. The chemical treatments affect the packing of the connexons in the crystal lattice (6), and could in turn alter the subunit structure of the connexon.

We found that the mild mechanical treatment yielded junctions with larger separations between connexons (~89 Å) than is obtained with conventional isolation procedures (where their center-to-center separation can be <80 Å [5, 6]). This is presumably because there is little or no extraction of the intervening lipid molecules. The larger separations and/or native lipid environment appears to allow the connexons to reside more symmetrically in the crystal lattice (evident from the good mirror symmetry in the diffraction patterns, Fig. 2)—a property of junctions treated with minimal amounts (6, 23), but not high concentrations of detergent (3).

To derive the three-dimensional map, data from individual images were combined according to the symmetry of the two-sided plane group p6, in a consistent orientation with respect to the electron source and carbon support film. This procedure led to similar amplitudes, but nearly opposite phases for the (1, 2) and (2, 1) lattice lines. If these junctions had a pronounced "sidedness," we would expect approximately equal numbers to be facing one way as facing the other (3, 6), and the derived (1, 2) and (2, 1) lattice lines to reflect the averaged Fourier terms, i.e., to have the same amplitudes and the same phases, but with more scatter in the phases. This is not the case, and the lattice line data therefore strongly suggest that the true crystallographic symmetry of these gap junctions is p622, with minor departures from this symmetry being a result of the asymmetric environment in which they are placed.

The connexon in the native membranes is an annular

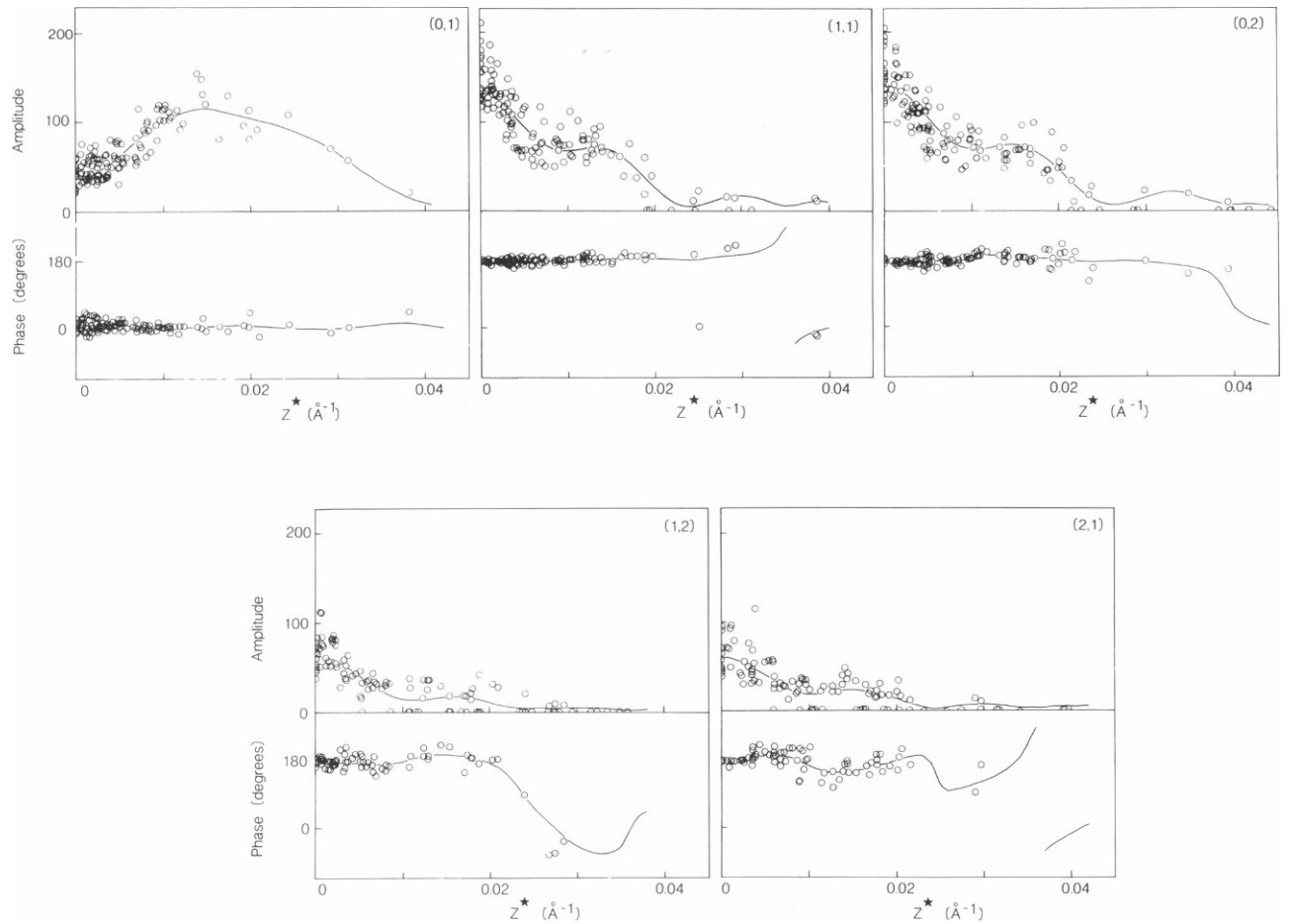


FIGURE 3. Experimental values and calculated curves tracing the continuous variation of amplitude and phase with distance, Z*, along the five major lattice lines. The data were combined assuming the symmetry of the two-sided plane group, p6, but similar amplitudes and opposite phases for the (1, 2) and (2, 1) lines indicate that the symmetry is a good approximation to p622.

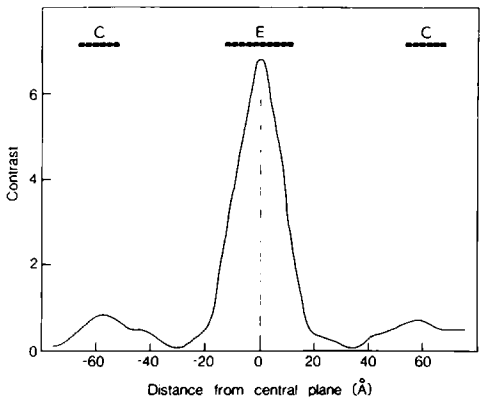


FIGURE 4. Plot of contrast (maximum density minus minimum density, excluding the region of the channel) in successive in-planar sections through the three-dimensional map. Regions corresponding to the extracellular (E) and cytoplasmic (C) portions of the structure are indicated. The contrast varies in a similar way in both halves of the junction, and is strongest in the extracellular space and at the cytoplasmic surface.

oligomer comprised of six rod-shaped subunits, which protrude from both membrane faces. The subunits extend ~15 Å from the extracellular face and rather less from the cytoplasmic face, although there could be more material here which is not visualized because of disorder (14) due, for example, to inhomogeneity of the protein (15). The path adopted by the subunits appears to be inclined slightly (5–10°) tangential to the central six-fold axis. There are small differences between connexons in the two apposed membranes, particularly at the cytoplasmic surfaces, which may simply be the result of small distortions associated with the unequal environment to which the two membranes have been exposed.

These three-dimensional features of the connexon are very similar to those shown by earlier electron microscopical analyses, using junctions treated with detergents and having smaller lattice dimensions (85 Å [20] and 80.6 Å [21], compared with 89 Å in this study). Previously, in the negative stain study (20), the tilting of the subunits was estimated to be 14° in one case and 9° in the other. The smaller inclination presumably relates most closely to the

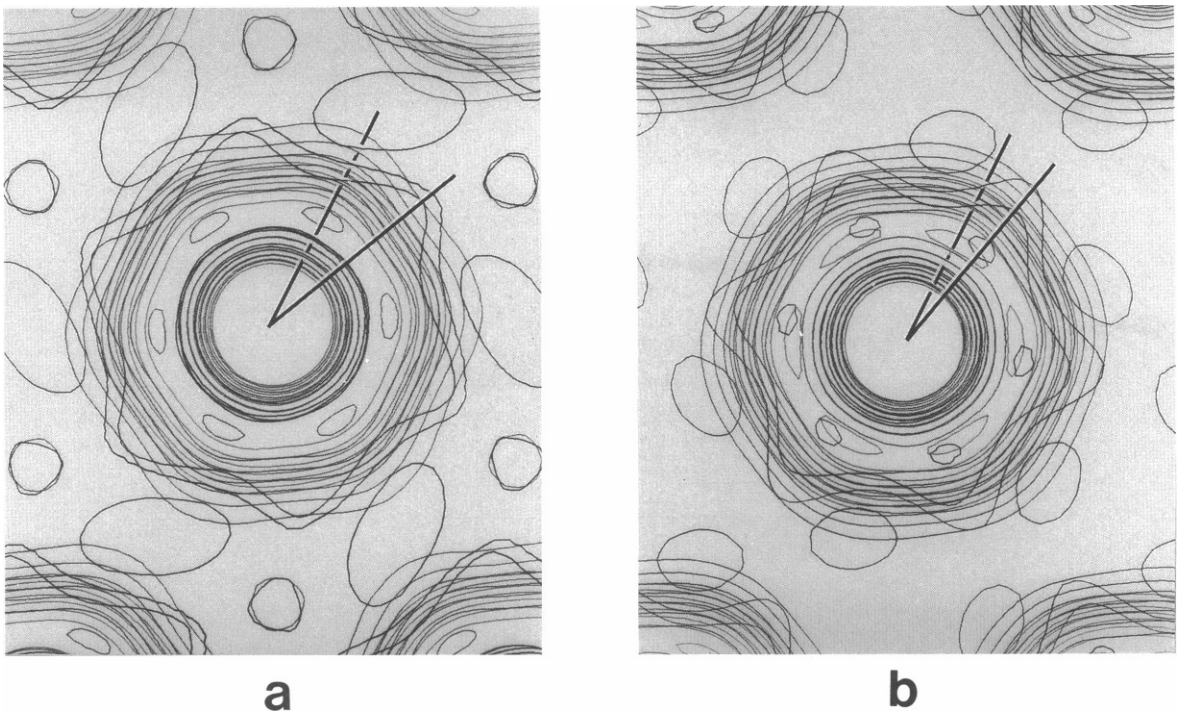


FIGURE 5. Superimposed sections from the three-dimensional map, illustrating the appearance of connexons in the upper (*a*) and lower (*b*) membranes of the gap junction. Both connexons are viewed as they would appear from the interior of the cell (i.e., darker cytoplasmic contours uppermost). Only the most strongly modulated sections (distances from central plane: 8, 12, 60, and 64 Å) are shown. Radial lines have been drawn in (*a*) and (*b*) to indicate the differences in azimuth of peaks in the modulations (i.e., subunit positions) on opposite sides of the membrane. Only the zero level and negative contours, corresponding to regions of greater stain exclusion, are shown. The outlines of the connexon are not accurately represented because the Fourier synthesis did not include terms from the lattice line through the origin (the [0, 0] lattice line).

present study, where $Ca^{2+}$ has been used to maintain the more compact configuration (21). However, only in this work has it been possible to visualise clearly the subunit details in both junctional membranes, and thus provide direct evidence for the symmetrical pairing of connexons in vivo.

This research was supported by a Muscular Dystrophy Association fellowship to Santosh Sikerwar, and grants GM27764 and GM30387 from the National Institutes of Health.

*Received for publication 20 November 1987 and in final form 21 March 1988.*

## REFERENCES

1. Agard, D. A. 1983. A least-squares method for determining structure factors in three-dimensional tilted-view reconstructions. *J. Mol. Biol.* 167:849–852.
2. Amos, L. A., R. Henderson, and P. N. T. Unwin. 1982. Three-dimensional structure determination by electron microscopy of two-dimensional crystals. *Prog. Biophys. Mol. Biol.* 39:183–231.
3. Baker, T. S., D. L. D. Caspar, C. J. Hollingshead, and D. A. Goodenough. 1983. Gap junction structures. IV. Asymmetric features revealed by low irradiation electron microscopy. *J. Cell Biol.* 96:204–216.
4. Brisson, A., and P. N. T. Unwin. 1985. Quaternary structure of the acetylcholine receptor. *Nature (Lond.).* 315:474–477.
5. Caspar, D. L. D., D. A. Goodenough, L. Makowski, and W. C. Phillips. 1977. Gap junction structures. I. Correlated electron microscopy and x-ray diffraction. *J. Cell. Biol.* 74:605–628.
6. Gogol, E. P., and P. N. T. Unwin. 1988. The organization of connexons in isolated rat liver gap junctions. *Biophys. J.* 54:105–112.
7. Goodenough, D. A., and W. Stoeckenius. 1972. The isolation of mouse hepatocyte gap junctions. *J. Cell Biol.* 54:646–656.
8. Hatefi, Y., and W. G. Hanstein. 1974. Destabilization of membranes with chaotropic ions. *Methods Enzymol.* 31:770–790.
9. Henderson, D., H. Eibl, and K. Weber. 1979. Structure and biochemistry of mouse hepatic gap junctions. *J. Mol. Biol.* 132:193–218.
10. Hertzberg, E. L. 1984. A detergent-independent procedure for the isolation of gap junctions from rat liver. *J. Biol. Chem.* 259:9936–9943.
11. Hertzberg, E. L., and N. B. Gilula. 1979. Isolation and characterization of gap junctions from rat liver. *J. Biol. Chem.* 254:2138–2147.
12. Makowski, L., D. L. D. Caspar, W. C. Phillips, and D. A. Goodenough. 1977. Gap junction structures. II. Analysis of the x-ray diffraction data. *J. Cell Biol.* 74:629–645.
13. Makowski, L., D. L. D. Caspar, W. C. Phillips, and D. A. Goodenough. 1984*a*. Gap junction structures. V. Structural chemistry inferred from x-ray diffraction measurements on sucrose accessibility and trypsin susceptibility. *J. Mol. Biol.* 174:449–481.
14. Makowski, L., D. L. D. Caspar, W. C. Phillips, T. S. Baker, and D. A. Goodenough. 1984*b*. Gap junction structures. VI. Variation and conservation in connexon conformation and packing. *Biophys. J.* 45:208–218.
15. Nicholson, B., R. Dermietzel, D. Teplow, O. Traub, K. Willecke, and

J.-P. Revel. 1987. Two homologous protein components of hepatic gap junctions. *Nature* (*Lond.*). 329:732–733.

16. Nicholson, B. J., and J. P. Revel. 1983. Gap junction in liver—Isolation, morphological analysis and quantitation. *Methods Enzymol.* 98:519–537.
17. Payton, B. W., M. V. L. Bennett, and G. D. Pappas. 1969. Permeability and structure of junctional membranes at an electrotonic synapse. *Science* (*Wash. DC*). 166:1642–1643.
18. Revel, J.-P., and J. J. Karnovsky. 1967. Hexagonal array of subunits in intercellular junctions of mouse heart and liver. *J. Cell Biol.* 33:C7–C12.
19. Robertson, J. D. 1963. The occurence of a subunit pattern in the unit membranes. *J. Cell Biol.* 19:201–221.
20. Unwin, P. N. T., and G. Zampighi. 1980. Structure of the junction between communicating cells. *Nature* (*Lond.*). 283:545–549.
21. Unwin, P. N. T., and P. D. Ennis. 1984. Two configurations of a channel-forming membrane protein. *Nature* (*Lond.*). 307:609–613.
22. Wrigley, N. G. 1968. The lattice spacing of crystalline catalase as an internal standard of length in electron microscopy. *J. Ultrastruct. Res.* 24:454–464.
23. Zampighi, G., and P. N. T. Unwin. 1979. Two forms of isolated gap junctions. *J. Mol. Biol.* 135:451–464.
24. Van Oostrum, J., P. R. Smith, M. Mohraz, and R. M. Burnett. 1987. The structure of the adenovirus capsid. III. Hexon packing determined from electron micrographs of capsid fragments. *J. Mol. Biol.* 198:73–89.